European Journal of Medicinal Chemistry 53 (2012) 168–175

Contents lists available at SciVerse ScienceDirect

European Journal of Medicinal Chemistry

journal homepage: http://www.elsevier.com/locate/ejmech

Original article

Synthesis, characterization and *in vitro* antitumour activity of a series of novel platinum(II) complexes bearing Schiff base ligands

Maria Proetto [a], Wukun Liu [a], Adelheid Hagenbach [b], Ulrich Abram [b], Ronald Gust [c,*]

[a] Institute of Pharmacy, Freie Universität Berlin, Königin-Luise-Str. 2+4, 14195 Berlin, Germany
[b] Institute of Chemistry and Biochemistry, Freie Universität Berlin, Fabeckstrasse 34-36, 14195 Berlin, Germany
[c] Institute of Pharmacy, University of Innsbruck, Innrain 80-82, A-6020 Innsbruck, Austria

ARTICLE INFO

Article history:
Received 22 November 2011
Received in revised form
20 March 2012
Accepted 27 March 2012
Available online 4 April 2012

Keywords:
Schiff base platinum complexes
Diarylsalene
Cytotoxicity
Synthesis

ABSTRACT

A series was neutral platinum(II) complexes bearing OCH_3- or F-substituted 3,4-bis(4-fluorophenyl)-1,6-bis(2-hydroxyphenyl)-2,5-diazahexa-1,5-dienes (diarylsalenes) were synthesized and tested for *in vitro* antitumour activity. The growth inhibitory effects depended on the configuration and the substitution pattern of the salicylidene moiety. The lead compound [*meso*-3,4-bis(4-fluorophenyl)-1,6-bis(2-hydroxyphenyl)-2,5-diazahexa-1,5-diene]platinum(II) (**1-Pt**) reduced the cell growth of MCF-7 (IC_{50} = 7.6 μM) and MDA-MB 231 cells (IC_{50} = 10.0 μM), but was inactive against HT-29 cells at the used concentration range (IC_{50} > 20 μM). The change of the configuration (*meso*→*d*,*l*) at the 1,2-diimino-1,2-diarylethane bridge and methoxy substitution led to completely inactive compounds, while fluorine substituents increased the antiproliferative effects depending on their position (3-F < 5-F < 4-F < 6-F). Complex **10-Pt** (6-F: IC_{50}(MCF-7) = 1.5 μM, IC_{50}(MDA-MB 231) = 1.3 μM, IC_{50} (HT-29) = 2.6 μM) was as active as cisplatin (IC_{50}(MCF-7) = 1.6 μM, IC_{50}(MDA-MB 231) = 1.5 μM, IC_{50}(HT-29) = 4.1 μM).

1. Introduction

Since the discovery of its biological activity in the early 1960s [1], cisplatin has become one of the most widely used and effective antineoplastic agents. Today, more than 30 years after approval, platinum-based drugs, e.g. cisplatin and carboplatin, still play a central role in cancer chemotherapy [2,3]. However, several disadvantages particularly related to general toxicity which leads to undesirable side effects and to drug-resistance phenomena limit their clinical use [4,5]. These restrictions and the fact that some tumoral diseases are not sensitive to platinum agents [3] forced the development of novel anticancer agents, combining platinum(II) with suitable carrier ligands [6–8].

Over the past years, promising results have been obtained for platinum complexes bearing a substituted 1,2-diaminoethane backbone (e.g. 1,2-diamino-1,2-diarylethane) as non-leaving group [7,9]. It has been shown that appropriate substituents on the aromatic rings could increase the cytotoxicity of the complexes. These interesting results induced us to synthesize platinum(II) complexes bearing Schiff base ligands derived from 1,2-diamino-1,2-diarylethanes and substituted salicylaldehydes. These Schiff bases (diarylsalenes) and others containing the N_2O_2 donor set are capable of forming stable complexes with transition metal ions (e.g. Co, Fe, Ni [10–13]; for a [diarylsalene]cobalt complexes see [14]).

Considering that in the diastereomeric [1,2-diamino-1,2-bis(4-fluorophenyl)ethane]platinum(II) complexes the neutral ligand has previously been identified as a carrier for the $PtCl_2$ moiety [15], **1-Pt** (see Scheme 1) was designed as lead compound for the [diarylsalene]platinum(II) series. Ligand modifications on **1-Pt** included *meso*→*d*,*l* stereomerization of the 1,2-diimino-1,2-diarylethane bridge (**2-Pt**, see Scheme 1) as well as OCH_3 and F substitution in the salicylidene moiety (**3-Pt** to **6-Pt**, and **7-Pt** to **10-Pt** respectively).

In vitro antitumour activities of the platinum compounds have been validated against the MCF-7 human breast cancer cell line and the effect of ligand substitution on cytotoxicity has been investigated. The most active compounds were additionally tested against MDA-MB 231 and HT-29 cells.

2. Results

2.1. Synthesis and structural characterization

The synthetic route to [diarylsalene]platinum(II) derivatives is outlined in Scheme 1. The Schiff bases were synthesized according

* Corresponding author. Tel.: +43 512 507 58200; fax: +43 512 507 58299.
E-mail address: ronald.gust@uibk.ac.at (R. Gust).

0223-5234/$ – see front matter © 2012 Elsevier Masson SAS. All rights reserved.
doi:10.1016/j.ejmech.2012.03.053

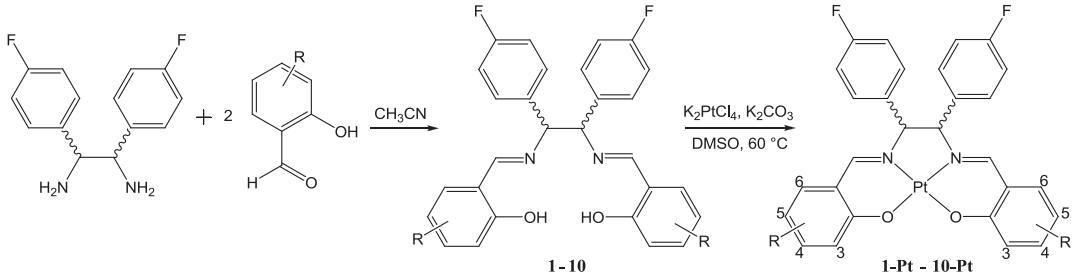

R	Config.	Compounds	R	Config.	Compounds
H	*meso*	**1**, **1-Pt**	6-OCH_3	*meso*	**6**, **6-Pt**
H	*d,l*	**2**, **2-Pt**	3-F	*meso*	**7**, **7-Pt**
3-OCH_3	*meso*	**3**, **3-Pt**	4-F	*meso*	**8**, **8-Pt**
4-OCH_3	*meso*	**4**, **4-Pt**	5-F	*meso*	**9**, **9-Pt**
5-OCH_3	*meso*	**5**, **5-Pt**	6-F	*meso*	**10**, **10-Pt**

Scheme 1. Synthetic route to [diarylsalene]platinum(II) complexes and their substitution patterns.

to a previously published method [14]. The diastereomerically pure 1,2-diamino-1,2-bis(4-fluorophenyl)ethanes [16–19] were reacted with two equivalents of the respective salicylaldehyde. The subsequent coordination to platinum was performed according to Tong et al. [20] with some modifications: the complexes were generated from the gently heated reaction mixture of the tetradentate ligands, potassium carbonate and potassium tetrachloroplatinate in DMSO.

The coordination was confirmed by NMR spectroscopy, mass spectrometry and X-ray crystallographic studies. In the case of the diarylsalene ligands, there is a free rotation around the central C–C bond. This leads to three staggered conformations: two structures with a *gauche*- and one with an *anti*-conformation. Previous crystallographic studies showed that 3,4-diaryl-1,6-bis(2-hydroxyphenyl)-2,5-diazahexa-1,5-diene in *meso*-configuration adapts an *anti*-conformation [21], in which the azomethine protons (NC*H*) are located above the aryl groups (Fig. 1) and suffer a shielding that reflects upfield of the signals of the above mentioned protons. This phenomenon was used to distinguish between *meso*- and *d*,*l*-isomers. The NC*H* protons of *d*,*l*-3,4-bis(4-fluorophenyl)-1,6-bis(2-hydroxyphenyl)-2,5-diazahexa-1,5-diene (**2**) which are not influenced in the same way showed a resonance in the ^{1}H NMR spectra at $\delta = 8.56$ (compared to $\delta = 8.45$ in **1**, see Fig. S1).

While the resonance of the azomethine proton was nearly identical for all *meso*-diarylsalenes ($\delta = 8.30$–8.70), the position (*ortho*, *meta* or *para*), much more than the kind of substituent (F or OCH_3) located at the salicylidene moiety, affected the OH signals

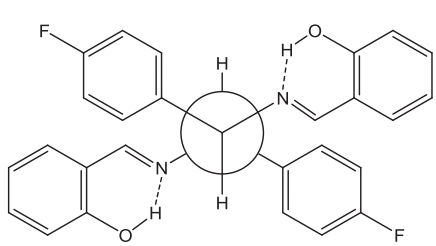

Fig. 1. Newman projection of **1** in the *anti*-conformation.

($\delta = 12.60$–14.30). It is important to emphasize that the resonance of the OH group is downfield-shifted relative to the signal for phenolic protons of regular H bonds [21]. This paramagnetic shift is as expected for Resonance-Assisted Hydrogen Bonds (RAHBs) [21,22]. Substituents (F or OCH_3) located in *ortho*- or *para*-position shifted the OH signal to a higher field (5: $\delta = 12.41$) compared to that of the *meta*-derivatives (6: $\delta = 13.97$) (Fig. S2). It is possible to compare the effects of fluorine and methoxy substitution for each position (Fig. S2: ligands **5** and **9**). We observed that an electron donating substituent like OCH_3 had a more pronounced shielding effect on the OH proton than F (**9**: $\delta = 12.68$) causing a larger diamagnetic shift (**5**: $\delta = 12.41$).

The coordination of the diarylsalene ligands to platinum(II), and the building of square-planar chelate complexes led to changes in the ^{1}H NMR spectra allowing the characterization of the compounds. The resonance signal of the phenolic OH groups completely disappeared upon coordination in all cases. This confirms the bonding of oxygen to the metal ions (C–O–M). The resonance signals of the 1,2-diarylethane moiety, as well as the signal of the NC*H* proton shifted in different directions (Fig. S3). Those of the aromatic protons and the azomethine proton suffered a diamagnetic shift, while the ones at the ethane bridge are paramagnetic shifted.

In addition, the ^{13}C NMR spectra of the selected compounds **1** and **1-Pt** were studied. Upon coordination of **1** to platinum(II) the azomethine carbons as well as the fluorine bound carbons (F–C_{Ar}) were upfield shifted, while the *CH* resonances of **1-Pt** appeared at lower field compared to **1**. Unlike the shifts observed in the ^{1}H NMR spectra, the changes in the ^{13}C NMR were only minimal.

The formation of complexes was further supported by positive mode ESI high resolution mass spectrometry, which documented a base peak corresponding to the $[M + Na]^+$ or $[M + K]^+$ ions.

To gain insight into the coordination chemistry and structural parameters of the [diarylsalene]platinum(II) complexes, **9-Pt** was isolated as single crystal by slow evaporation of a concentrated methanol solution and was characterized by X-ray diffraction. Its crystal structure is shown in Fig. 2 together with the numbering scheme for the atoms.

A summary of crystal data, experimental details and refinement methods are given in Table 1.

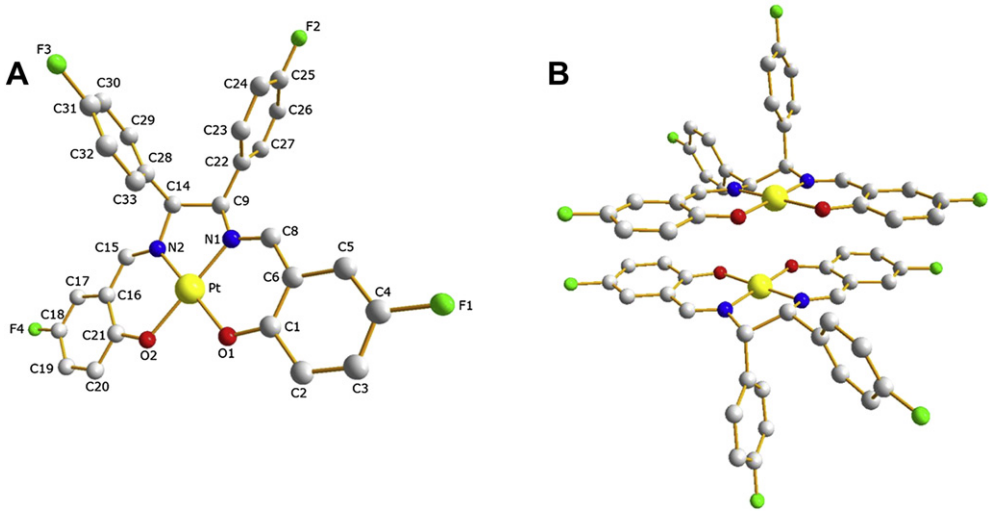

Fig. 2. A: X-ray molecular structure of **9-Pt**. The hydrogen atoms are omitted for clarity. B: Crystal packing diagram of **9-Pt**, where complexes are arranged in pairs and in a head-to-tail fashion.

The crystal structure shows that in **9-Pt** the Schiff base ligand (**9**) is four-fold coordinated at the platinum(II) *via* the azomethine nitrogens and the oxygen atom of the hydroxyl groups. The platinum atom resides in a square-planar geometry. The bond angles at the platinum atom (N1–Pt–N2, N1–Pt–O1, N2–Pt–O2 and O1–Pt–O2) lie in the range of 85.0–94.9°. The average Pt–N and Pt–O distances of 1.927 and 1.991 Å respectively, resemble those reported for similar platinum(II) complexes bearing the N_2O_2 ligand donor set [23–25].

Concerning the crystal packing, the molecules seem to be arranged in a head-to-tail fashion with intermolecular π–π stacking interactions mainly between the salicylidene moieties (see Fig. 2 right).

2.2. Antiproliferative effects

The [diarylsalene]platinum(II) complexes and the established antitumour drug cisplatin were tested for *in vitro* activity against MCF-7 human breast cancer cells. IC_{50} values determined after 96 h of incubation are shown in Table 2. The most active compounds were additionally tested against MDA-MB 231 and HT-29 cells.

Variations on the salicylidene moiety determined the activity of the complexes at the MCF-7 cell line. On the one hand, the introduction of methoxy groups gave inactive compounds at the used concentrations. On the other hand, the substitution with fluorines resulted in active complexes in which the IC_{50} values depended on the F-position on the ring. While 3-F substitution (**7-Pt**) led to a complex which did not influence the tumour cell growth, the shift of the fluorine from the 3- into the 6-position (**10-Pt**) enormously increased the antiproliferative effects. Complex **10-Pt** (IC_{50} = 1.5 μM) was not only more active than the lead compound **1-Pt**, but caused cytotoxicity comparable to that of cisplatin (IC_{50} = 1.6 μM). The isomers **8-Pt** (4-F) and **9-Pt** (5-F) reduced the growth of MCF-7 cells to a much lower extend (IC_{50} = 7.8 and 12.7 μM). It is interesting to note that the *meso*→*d*,*l* stereoisomerization of the 1,2-diimino-1,2-diarylethane bridge led to inactive compounds within the tested range of concentrations.

Substances which presented IC_{50} values <20 μM were time-dependently tested for growth inhibitory effects against MCF-7 cells (Fig. 3) and for cytotoxicity (IC_{50}) against MDA-MB 231 and HT-29 cells (Table 2).

In contrast to cisplatin, which reached its maximum effect towards the end of the test (Fig. S4), the onset of activity of the [diarylsalene]platinum(II) complexes was observed earlier (48–72 h) occasionally followed by a recuperation of the cells. In the case of **1-Pt**, the cell population already started to recover after the initial damage. Because exponential cell growth is guaranteed for at least 250 h of incubation, the rise of the growth curve can be explained by the development of drug-resistance [26]. The recovery is also observed for **9-Pt** and at low concentrations (0.63 and 1.25 μM) for **10-Pt**.

It is worthy to mention that **10-Pt** caused cytocidal effects ($T/C_{corr} < 0\%$) at concentrations of 5 and 10 μM which can be hold until the end of the experiment. Such growth inhibition could not be observed with cisplatin (Fig. S4).

At the MDA-MB 231 cell line (Table 2), **1-Pt** (IC_{50} = 10.0 μM), **8-Pt** (IC_{50} = 5.3 μM) and **10-Pt** (IC_{50} = 1.3 μM) were as active as against MCF-7 cells, while **9-Pt** was inactive (IC_{50} > 20 μM). Interestingly, only **8-Pt** (IC_{50} = 6.7 μM) and **10-Pt** (IC_{50} = 2.6 μM)

Table 1
Crystal data and structure refinement for **9-Pt**.

Crystal system	Monoclinic	
Space group	$P2_1/n$	
Unit cell dimensions	a (Å) 12.075(2)	α (°) 90.00(1)
	b (Å) 18.559(2)	β (°) 107.27(1)
	c (Å) 11.839(2)	γ (°) 11.84(1)
V (Å^3)	2533.5(7)	
Z	4	
ρ_{calcd} (g cm^{-3})	1.860	
μ ($Mo_{K\alpha}$) (mm^{-1})	5.602	
F(000)	1372	
Crystal colour	Yellow	
Crystal shape	Block	
Crystal size (mm^3)	0.16 × 0.12 × 0.10	
Reflections collected	14473	
Independent reflections	6755 (R_{int} = 0.1085)	
Absorption correction	Integration	
Max. and min. transmission	0.6083 and 0.4751	
Refinement method	Full-matrix least-squares on F^2	
Data/restrains/parameters	6755/0/346	
Goodness of fit on F^2	0.670	
Final R indices [I > 2σ(I)]	R_1 = 0.0428, wR_2 = 0.0601	
R indices (all data)	R_1 = 0.1560, wR_2 = 0.0757	
Largest diff. peak and hole (e Å^{-3})	1.656 and −1.723	
Deposit number	CCDC-859077	

Table 2
Cytotoxicity (IC_{50} values [μM]) of [diarylsalene]platinum(II) complexes on the MCF-7 and MDA-MB 231 breast cancer as well as HT-29 colon carcinoma cell lines.[a]

	MCF-7	MDA-MB 231	HT-29		MCF-7	MDA-MB 231	HT-29
1-Pt	7.6 ± 2.9	10.0 ± 1.7	>20.0	**7-Pt**	>20.0	nd[b]	nd[b]
2-Pt	>20.0	nd[b]	nd[b]	**8-Pt**	7.8 ± 1.1	5.3 ± 2.0	6.7 ± 1.3
3-Pt	>20.0	nd[b]	nd[b]	**9-Pt**	12.7 ± 2.0	>20.0	>20.0
4-Pt	>20.0	nd[b]	nd[b]	**10-Pt**	1.5 ± 0.1	1.3 ± 0.3	2.6 ± 0.5
5-Pt	>20.0	nd[b]	nd[b]	**Cisplatin**	1.6 ± 0.1	1.5 ± 0.1	4.1 ± 0.3
6-Pt	>20.0	nd[b]	nd[b]				

[a] The IC_{50} values represent the concentration results in a 50% decrease in cell growth after 96 h incubation and was calculated as mean of at least two independent experiments.
[b] nd: Not determined.

reduced the growth of HT-29 cells. This might be an indication that the substituents at the salicylidene moiety can also determine tumour selectivity which however must be confirmed in an extended SAR study. Furthermore, it would be of interest to study especially the effects of **10-Pt** against cisplatin-resistant cells. This complex was active at all cell lines used; at HT-29 cells it was even more potent than cisplatin.

3. Discussion

The synthesized [diarylsalene]platinum(II) complexes displayed cytotoxic potency against MCF-7 and MDA-MB 231 human breast cancer as well as against HT-29 colon carcinoma cells, depending on the configuration and substitution pattern of the ligands. The configuration of the 1,2-diimino-1,2-diarylethane bridge played an essential role. Replacement of the *meso*-configured ligand of the lead structure **1-Pt** with its *d*,*l*-configured isomer led to a completely inactive compound (**2-Pt**) at the tested range of concentrations. It has been recently observed for similar substituted [diarylsalene]cobalt complexes, that the respective *meso*-configured compounds were enriched in higher amounts in the tumour cells than the corresponding *d*,*l*-configured complexes [14], and therefore a carrier mediated cellular uptake has been proposed. Considering the similarities between ligands of the reported cobalt and our synthesized platinum complexes, it is reasonable to propose that the observed inactivity of **2-Pt** is due to decreased cellular accumulation (when compared to **1-Pt**).

The influence of a substituted salicylidene moiety on cytotoxicity is pronounced and modulated the activity. While the incorporation of methoxy groups drastically reduced the *in vitro* antitumour effects, complexes bearing a fluorine-substituted salicylidene moiety presented variable cytotoxic activity

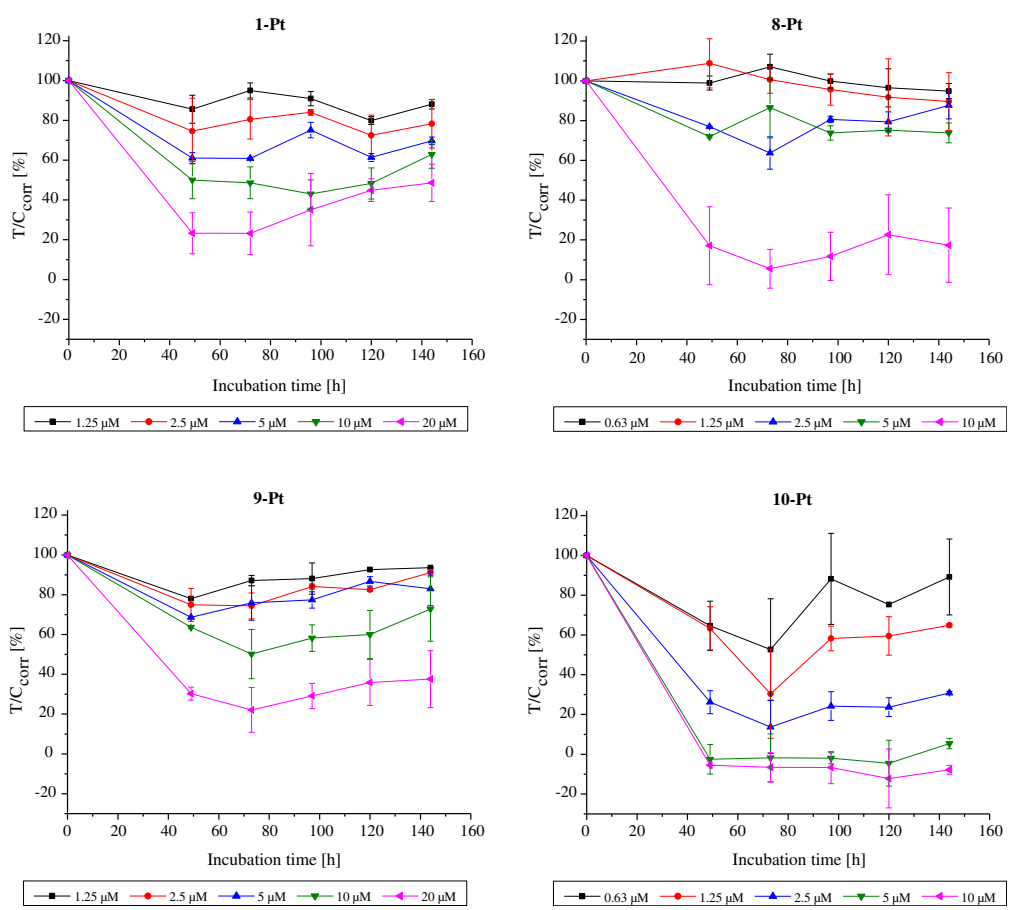

Fig. 3. Time-dependent antiproliferative effects of **1-Pt**, **8-Pt**, **9-Pt** and **10-Pt** on MCF-7 cells.

depending on the position of the substituent. It has been demonstrated by ^{1}H NMR spectroscopy that electron donating groups (e.g. OCH_3) have more pronounced shielding effects on the OH proton than fluorine substituents, when a specific ring position is compared. If this effect is due to the changed electron density at the oxygen atom, it might have also an influence on the respective Pt–O bond. Thus, the low activity of the methoxy-substituted complexes could be explained by the strengthening of the Pt–O bond, the increase of energy needed for a ring opening and therefore, the decrease in reactivity towards its proposed target, the DNA. Nevertheless, this effect cannot be generalized. While the ^{1}H NMR resonance signals of the hydroxyl groups are much more affected by the position than by the kind of substituent, the growth inhibitory effects depend mainly on the kind of substituents at the 1,2-diarylethane.

4. Conclusion

Novel [diarylsalene]platinum(II) complexes were successfully synthesized and characterized. It has been demonstrated that substitution with electron donation groups terminates the cytotoxic activity, while fluorine substitution can enhance the antiproliferative effects. It is presumed that these effects could be partially originated by changes on reactivity of the complexes related to the electron density on the Pt–O bonds. However, the missing correlation between this expected reactivity and the cytotoxicity evidences the involvement of more specific processes or interactions of the complexes outside or inside the tumour cells. Further experiments related to the target of the complexes (such as DNA interaction studies) and to the intracellular accumulation (drug uptake/efflux studies) will help to clarify to influence of the substituents on the cytotoxic effects.

5. Experimental section

5.1. General procedures

The following instrumentation was used: ^{1}H NMR spectra: Bruker ADX 400 spectrometer operated at 400 MHz (internal standard, tetramethylsilane); ESI-TOF spectra: Agilent 6210 ESI-TOF, Agilent Technologies, Santa Clara, CA, USA. Chemicals were obtained from Sigma–Aldrich (Germany) and used without further purification. The 1,2-diamino-1,2-diarylethanes were synthesized as described earlier [16–19]. Reactions were all monitored by TLC, performed on silica gel plates 60 F254 (Merck, Darmstadt/Germany). Visualization on TLC was achieved by UV light.

5.2. Syntheses

5.2.1. General procedure for the synthesis of meso- and d,l-3,4-bis(4-fluorophenyl)-1,6-bis(2-hydroxyphenyl)-2,5-diazahexa-1,5-diene derivatives

An amount of one equivalent of the respective 1,2-diamino-1,2-diarylethane was suspended in acetonitrile and reacted with two equivalents of the respective salicylaldehyde. The reaction mixture was heated to reflux for 6 h. The solvent was reduced by half, and the diimine was subsequently allowed to crystallize. The crystals were filtered off, washed with diethyl ether, and dried over P_2O_5.

*5.2.1.1. meso-3,4-Bis(4-fluorophenyl)-1,6-bis(2-hydroxyphenyl)-2,5-diazahexa-1,5-diene [**1**].* **1** was obtained from *meso*-1,2-diamino-1,2-bis(4-fluorophenyl)ethane (0.40 mmol, 99 mg) and salicylaldehyde (0.80 mmol, 98 mg). Yield: 166 mg (0.36 mmol, 91%) of yellow crystals. ^{1}H NMR (DMSO-d_6): δ = 5.09 (s, 2H, C*H*); 6.82–6.92 (m, 4H, Ar*H*-3, Ar*H*-5); 7.10–7.22 (t, ^3J = 8.81 Hz, 4H, Ar′*H*-3, Ar′*H*-5); 7.27–7.41 (m, 8H, Ar*H*-4, Ar*H*-6, Ar′*H*-2, Ar′*H*-6); 8.45 (s, 2H, NC*H*); 13.03 (s, 2H, ArO*H*). ^{13}C NMR (DMSO-d_6): δ = 166.94 (C=N); 160.67, 160.20 (F–C_{Ar}); 136.60 (d); 133.24, 132.40, 130.33 (d), 119.39, 119.04, 116.95, 115.78, 115.57 (C_{Ar}); 77.25 (CH).

*5.2.1.2. d,l-3,4-Bis(4-fluorophenyl)-1,6-bis(2-hydroxyphenyl)-2,5-diazahexa-1,5-diene [**2**].* **2** was obtained from *d,l*-1,2-diamino-1,2-bis(4-fluorophenyl)ethane (3.98 mmol, 989 mg) and salicylaldehyde (7.97 mmol, 972 mg). Yield: 1.3 g (2.85 mmol, 72%) of yellow crystals. ^{1}H NMR (DMSO-d_6): δ = 5.11 (s, 2H, C*H*); 6.81–6.89 (m, 4H, Ar*H*-3, Ar*H*-5); 7.07–7.15 (t, ^3J = 8.81 Hz, 4H, Ar′*H*-3, Ar′*H*-5); 7.27–7.38 (m, 8H, Ar*H*-4, Ar*H*-6, Ar′*H*-2, Ar′*H*-6); 8.56 (s, 2H, NC*H*); 13.15 (s, 2H, ArO*H*).

*5.2.1.3. meso-3,4-Bis(4-fluorophenyl)-1,6-bis(2-hydroxy-3-methoxyphenyl)-2,5-diazahexa-1,5-diene [**3**].* **3** was obtained from *meso*-1,2-diamino-1,2-bis(4-fluorophenyl)ethane (0.35 mmol, 86 mg) and 3-methoxysalicylaldehyde (0.69 mmol, 97 mg). Yield: 129 mg (0.26 mmol, 75%) of light yellow crystals. ^{1}H NMR (DMSO-d_6): δ = 3.77 (s, 6H, OCH_3); 5.08 (s, 2H, C*H*); 6.76–6.84 (t, 2H, ^3J = 7.87 Hz, Ar*H*-5); 6.87–6.97 (dd, ^3J = 7.90 Hz, ^4J = 1.30 Hz, 2H, Ar*H*-4); 7.00–7.08 (dd, ^3J = 8.00 Hz, ^4J = 1.20 Hz, 2H, Ar*H*-6); 7.12–7.21 (t, ^3J = 8.81 Hz, 4H, Ar′*H*-3, Ar′*H*-5); 7.30–7.44 (m, 4H, Ar′*H*-2, Ar′*H*-6); 8.44 (s, 2H, NC*H*); 13.21 (s, 2H, ArO*H*).

*5.2.1.4. meso-3,4-Bis(4-fluorophenyl)-1,6-bis(2-hydroxy-4-methoxyphenyl)-2,5-diazahexa-1,5-diene [**4**].* **4** was obtained from *meso*-1,2-diamino-1,2-bis(4-fluorophenyl)ethane (0.18 mmol, 44 mg) and 4-methoxysalicylaldehyde (0.35 mmol, 53 mg). Yield: 70 mg (0.14 mmol, 75%) of yellow crystals. ^{1}H NMR (DMSO-d_6): δ = 3.75 (s, 6H, CH_3); 4.98 (s, 2H, C*H*); 6.36–6.40 (d, ^4J = 2.28 Hz, 2H, Ar*H*-3); 6.40–6.45 (dd, ^3J = 8.54 Hz, ^4J = 2.36 Hz, 2H, Ar*H*-5); 7.10–7.19 (t, ^3J = 8.81 Hz, 4H, Ar′*H*-3, Ar′*H*-5); 7.19–7.25 (d, ^3J = 8.57 Hz, 2H, Ar*H*-6); 7.26–7.34 (m, 4H, Ar′*H*-2, Ar′*H*-6); 8.32 (s, 2H, NC*H*); 13.54 (s, 2H, ArO*H*).

*5.2.1.5. meso-3,4-Bis(4-fluorophenyl)-1,6-bis(2-hydroxy-5-methoxyphenyl)-2,5-diazahexa-1,5-diene [**5**].* **5** was obtained from *meso*-1,2-diamino-1,2-bis(4-fluorophenyl)ethane (0.22 mmol, 55 mg) and 5-methoxysalicylaldehyde (0.44 mmol, 67 mg). Yield: 90 mg (0.17 mmol, 79%) of yellow crystals. ^{1}H NMR (DMSO-d_6): δ = 3.67 (s, 6H, CH_3); 5.06 (s, 2H, C*H*); 6.77–6.83 (d, ^3J = 8.47 Hz, 2H, Ar*H*-3); 6.90–6.99 (m, 4H, Ar*H*-4, Ar*H*-6); 7.12–7.21 (t, ^3J = 8.77 Hz, 4H, Ar′*H*-3, Ar′*H*-5); 7.30–7.39 (m, 4H, Ar′*H*-2, Ar′*H*-6); 8.41 (s, 2H, NC*H*); 12.41 (s, 2H, ArO*H*).

*5.2.1.6. meso-3,4-Bis(4-fluorophenyl)-1,6-bis(2-hydroxy-6-methoxyphenyl)-2,5-diazahexa-1,5-diene [**6**].* **6** was obtained from *meso*-1,2-diamino-1,2-bis(4-fluorophenyl)ethane (0.54 mmol, 133 mg) and 6-methoxysalicylaldehyde (1.07 mmol, 163 mg). Yield: 226 mg (0.44 mmol, 83%) of yellow crystals. ^{1}H NMR (DMSO-d_6): δ = 3.75 (s, 6H, CH_3); 5.16 (s, 2H, C*H*); 6.37–6.49 (m, 4H, Ar*H*-3, Ar*H*-5); 7.12–7.21 (t, ^3J = 8.82 Hz, 4H, Ar′*H*-3, Ar′*H*-5); 7.23–7.29 (t, 2H, ^3J = 8.82 Hz, Ar*H*-4); 7.31–7.39 (m, 4H, Ar′*H*-2, Ar′*H*-6); 8.70 (s, 2H, NC*H*); 13.97 (s, 2H, ArO*H*).

*5.2.1.7. meso-3,4-Bis(4-fluorophenyl)-1,6-bis(2-hydroxy-3-fluorophenyl)-2,5-diazahexa-1,5-diene [**7**].* **7** was obtained from *meso*-1,2-diamino-1,2-bis(4-fluorophenyl)ethane (0.35 mmol, 86 mg) and 3-fluorosalicylaldehyde (0.69 mmol, 97 mg). Yield: 129 mg (0.26 mmol, 75%) of light yellow crystals. ^{1}H NMR (DMSO-d_6): δ = 5.18 (s, 2H, C*H*); 6.80–6.88 (m, 2H, Ar*H*-5); 7.15–7.23 (m, 6H, Ar*H*-6, Ar′*H*-3, Ar′*H*-5); 7.26–7.35 (m, 2H, Ar*H*-4); 7.35–7.44 (m, 4H, Ar′*H*-2, Ar′*H*-6); 8.49 (s, 2H, NC*H*); 13.51 (s, 2H, ArO*H*).

*5.2.1.8. meso-3,4-Bis(4-fluorophenyl)-1,6-bis(2-hydroxy-4-fluorophenyl)-2,5-diazahexa-1,5-diene [**8**].* **8** was obtained from *meso*-1,2-diamino-1,2-bis(4-fluorophenyl)ethane (0.41 mmol, 104 mg) and 4-fluorosalicylaldehyde (0.84 mmol, 117 mg). Yield: 161 mg (0.33 mmol, 80%) of a light yellow powder. ^{1}H NMR (DMSO-d_6): $\delta = 5.08$ (s, 2H, C*H*); 6.65–6.75 (m, 4H, Ar*H*-3, Ar*H*-5); 7.11–7.21 (t, $^3J = 8.80$ Hz, 4H, Ar′*H*-3, Ar′*H*-5); 7.30–7.36 (m, 4H, Ar′*H*-2, Ar′*H*-6); 7.39–7.46 (m, 2H, Ar*H*-6); 8.44 (s, 2H, NC*H*); 13.69 (s, 2H, ArO*H*).

*5.2.1.9. meso-3,4-Bis(4-fluorophenyl)-1,6-bis(2-hydroxy-5-fluorophenyl)-2,5-diazahexa-1,5-diene [**9**].* **9** was obtained from *meso*-1,2-diamino-1,2-bis(4-fluorophenyl)ethane (0.34 mmol, 85 mg) and 5-fluorosalicylaldehyde (0.68 mmol, 95 mg). Yield: 110 mg (0.22 mmol, 66%) of dark yellow crystals. ^{1}H NMR (DMSO-d_6): $\delta = 5.09$ (s, 2H, C*H*); 6.85–6.91 (dd, $^3J = 9.01$ Hz, $^4J = 4.05$ Hz, 2H, Ar*H*-3); 7.08–7.23 (m, 6H, Ar*H*-4, Ar′*H*-3, Ar′*H*-5); 7.23–7.29 (dd, $^3J = 8.85$ Hz, $^4J = 3.11$ Hz, 2H, Ar*H*-6); 7.29–7.42 (m, 4H, Ar′*H*-2, Ar′*H*-6); 8.41 (s, 2H, NC*H*); 12.68 (s, 2H, ArO*H*).

*5.2.1.10. meso-3,4-Bis(4-fluorophenyl)-1,6-bis(2-hydroxy-6-fluorophenyl)-2,5-diazahexa-1,5-diene [**10**].* **10** was obtained from *meso*-1,2-diamino-1,2-bis(4-fluorophenyl)ethane (0.35 mmol, 89 mg) and 6-fluorosalicylaldehyde (0.71 mmol, 100 mg). Yield: 75 mg (0.15 mmol, 43%) of yellow crystals. ^{1}H NMR (DMSO-d_6): $\delta = 5.28$ (s, 2H, C*H*); 6.62–6.75 (m, 4H, Ar*H*-3, Ar*H*-5); 7.15–7.24 (t, $^3J = 8.81$ Hz, 4H, Ar′*H*-3, Ar′*H*-5); 7.32–7.42 (m, 6H, Ar*H*-4, Ar′*H*-2, Ar′*H*-6); 8.67 (s, 2H, NC*H*); 13.70 (s, 2H, ArO*H*).

5.2.2. General procedure for the synthesis of the [3,4-bis(4-fluorophenyl)-1,6-bis(2-hydroxyphenyl)-2,5-diazahexa-1,5-diene] platinum(II) complexes

Two equivalents of K_2CO_3 were dissolved in water, and the resulting solution was added slowly to a solution of one equivalent of the ligand in dry DMSO. Afterwards, a solution of one equivalent of potassium tetrachloroplatinate in water was added dropwise. The mixture was heated for 5 h, keeping the temperature of the reaction below 60 °C. The mixture was allowed to cool to room temperature and the solid matter was filtered off.

*5.2.2.1. [meso-3,4-Bis(4-fluorophenyl)-1,6-bis(2-hydroxyphenyl)-2,5-diazahexa-1,5-diene]platinum(II) [**1-Pt**].* **1-Pt** was obtained from *meso*-3,4-bis(4-fluorophenyl)-1,6-bis(2-hydroxyphenyl)-2,5-diazahexa-1,5-diene (**1**) (0.20 mmol, 91 mg) and potassium tetrachloroplatinate (0.20 mmol, 82 mg). Yield: 69 mg (0.11 mmol, 53%) of a yellow powder. ^{1}H NMR (DMSO-d_6): $\delta = 5.55$ (s, 2H, C*H*); 6.53–6.63 (t, $^3J = 7.27$ Hz, 2H, Ar*H*-5); 6.95–7.03 (d, $^3J = 8.53$ Hz, 2H, Ar*H*-3); 7.07–7.15 (t, $^3J = 8.79$ Hz, 4H, Ar′*H*-3, Ar′*H*-5); 7.20–7.27 (m, 4H, Ar′*H*-2, Ar′*H*-6); 7.39–7.52 (m, 4H, Ar*H*-4, Ar*H*-6); 8.26 (s, 2H, NC*H*). ^{13}C NMR ([D7]DMF): $\delta = 163.6$, 163.4 (C=N); 156.8, 156.7 (F–C_{Ar}); 134.6, 134.4, 134.3, 134.2, 131.7, 122.9, 121.5, 121.3, 115.9, 115.8, 115.5, 115.4 (C_{Ar}); 79.1, 79.0 (CH). HRMS (+)-ESI *m*/*z* [M + Na]$^+$ calcd for $C_{28}H_{20}F_2N_2NaO_2Pt^+$: 672.1038; found: 672.1001.

*5.2.2.2. [d,l-3,4-Bis(4-fluorophenyl)-1,6-bis(2-hydroxyphenyl)-2,5-diazahexa-1,5-diene]platinum(II) [**2-Pt**].* **2-Pt** was obtained from *d,l*-3,4-bis(4-fluorophenyl)-1,6-bis(2-hydroxyphenyl)-2,5-diazahexa-1,5-diene (**2**) (0.20 mmol, 91 mg) and potassium tetrachloroplatinate (0.20 mmol, 82 mg). Yield: 98 mg (0.15 mmol, 75%) of a yellow powder. ^{1}H NMR (DMSO-d_6): $\delta = 5.28$ (s, 2H, C*H*); 6.56–6.67 (t, $^3J = 7.34$ Hz, 2H, Ar*H*-5); 6.93–7.02 (d, $^3J = 7.41$ Hz, 2H, Ar*H*-3); 7.22–7.34 (t, $^3J = 8.81$ Hz, 4H, Ar′*H*-3, Ar′*H*-5); 7.40–7.54 (m, 4H, Ar*H*-4, Ar*H*-6); 7.69–7.83 (m, 4H, Ar′*H*-2, Ar′*H*-6); 8.52 (s, 2H, NC*H*). HRMS (+)-ESI *m*/*z* [M + Na]$^+$ calcd for $C_{28}H_{20}F_2N_2NaO_2Pt^+$: 672.1038; found: 672.1004.

*5.2.2.3. [meso-3,4-Bis(4-fluorophenyl)-1,6-bis(2-hydroxy-3-methoxyphenyl)-2,5-diazahexa-1,5-diene]platinum(II) [**3-Pt**].* **3-Pt** was obtained from *meso*-3,4-bis(4-fluorophenyl)-1,6-bis(2-hydroxy-3-methoxyphenyl)-2,5-diazahexa-1,5-diene (**3**) (0.19 mmol, 137 mg) and potassium tetrachloroplatinate (0.19 mmol, 79 mg). Yield: 79 mg (0.11 mmol, 61%) of a yellow powder. ^{1}H NMR (DMSO-d_6): $\delta = 3.82$ (s, 6H, OCH_3); 5.54 (s, 2H, C*H*); 6.48–6.56 (t, 2H, $^3J = 7.84$ Hz, Ar*H*-5); 6.96–7.02 (m, 2H, Ar*H*-4); 7.06–7.25 (m, 10H, Ar*H*-6, Ar′*H*-2, Ar′*H*-3, Ar′*H*-5, Ar′*H*-6); 8.23 (s, 2H, NC*H*). HRMS (+)-ESI *m*/*z* [M + K]$^+$ calcd for $C_{30}H_{24}F_2KN_2O_4Pt^+$: 748.0989; found: 748.1033.

*5.2.2.4. [meso-3,4-Bis(4-fluorophenyl)-1,6-bis(2-hydroxy-4-methoxyphenyl)-2,5-diazahexa-1,5-diene]platinum(II) [**4-Pt**].* **4-Pt** was obtained from *meso*-3,4-bis(4-fluorophenyl)-1,6-bis(2-hydroxy-4-methoxyphenyl)-2,5-diazahexa-1,5-diene (**4**) (0.08 mmol, 44 mg) and potassium tetrachloroplatinate (0.08 mmol, 35 mg). Yield: 20 mg (0.03 mmol, 35%) of a yellow powder. ^{1}H NMR (DMSO-d_6): $\delta = 3.77$ (s, 6H, CH_3); 5.45 (s, 2H, C*H*); 6.20–6.26 (dd, $^3J = 8.81$ Hz, $^4J = 2.28$ Hz, 2H, Ar*H*-5); 6.46–6.50 (d, $^4J = 2.21$ Hz, 2H, Ar*H*-3); 7.05–7.13 (t, $^3J = 8.76$ Hz, 4H, Ar′*H*-3, Ar′*H*-5); 7.17–7.24 (m, 4H, Ar′*H*-2, Ar′*H*-6); 7.27–7.32 (d, $^3J = 8.88$, 2H, Ar*H*-6); 8.05 (s, 2H, NC*H*). HRMS (+)-ESI *m*/*z* [M + K]$^+$ calcd for $C_{30}H_{24}F_2KN_2O_4Pt^+$: 748.0989; found: 748.0999.

*5.2.2.5. [meso-3,4-Bis(4-fluorophenyl)-1,6-bis(2-hydroxy-5-methoxyphenyl)-2,5-diazahexa-1,5-diene]platinum(II) [**5-Pt**].* **5-Pt** was obtained from *meso*-3,4-bis(4-fluorophenyl)-1,6-bis(2-hydroxy-5-methoxyphenyl)-2,5-diazahexa-1,5-diene (**5**) (0.10 mmol, 54 mg) and potassium tetrachloroplatinate (0.10 mmol, 43 mg). Yield: 25 mg (0.03 mmol, 35%) of a yellow powder. ^{1}H NMR (DMSO-d_6): $\delta = 3.63$ (s, 6H, CH_3); 5.53 (s, 2H, C*H*); 6.89–6.94 (d, $^3J = 9.23$ Hz, 2H, Ar*H*-3); 6.95–6.98 (d, $^4J = 3.14$ Hz, 2H, Ar*H*-6); 7.08–7.19 (m, 6H, Ar*H*-4, Ar′*H*-3, Ar′*H*-5); 7.19–7.26 (m, 4H, Ar′*H*-2, Ar′*H*-6); 8.24 (s, 2H, NC*H*). HRMS (+)-ESI *m*/*z* [M + Na]$^+$ calcd for $C_{30}H_{24}F_2N_2NaO_4Pt^+$: 732.1250; found: 732.1246.

*5.2.2.6. [meso-3,4-Bis(4-fluorophenyl)-1,6-bis(2-hydroxy-6-methoxyphenyl)-2,5-diazahexa-1,5-diene]platinum(II) [**6-Pt**].* **6-Pt** was obtained from *meso*-3,4-bis(4-fluorophenyl)-1,6-bis(2-hydroxy-6-methoxyphenyl)-2,5-diazahexa-1,5-diene (**6**) (0.32 mmol, 163 mg) and potassium tetrachloroplatinate (0.32 mmol, 130 mg). Yield: 30 mg (0.04 mmol, 13%) of a brown powder. ^{1}H NMR (DMSO-d_6): $\delta = 3.73$ (s, 6H, CH_3); 5.42 (s, 2H, C*H*); 6.13–6.22 (d, $^3J = 7.91$ Hz, 2H, Ar*H*-5); 6.53–6.58 (d, $^3J = 8.68$ Hz, 2H, Ar*H*-3); 7.23–7.30 (t, $^3J = 8.84$ Hz, 4H, Ar′*H*-3, Ar′*H*-5); 7.31–7.37 (t, $^3J = 8.33$, 2H, Ar*H*-4); 7.69–7.75 (m, 4H, Ar′*H*-2, Ar′*H*-6); 8.75 (s, 2H, NC*H*). HRMS (+)-ESI *m*/*z* [M + K]$^+$ calcd for $C_{30}H_{24}F_2KN_2O_4Pt^+$: 748.0989; found: 748.0965.

*5.2.2.7. [meso-3,4-Bis(4-fluorophenyl)-1,6-bis(2-hydroxy-3-fluorophenyl)-2,5-diazahexa-1,5-diene]platinum(II) [**7-Pt**].* **7-Pt** was obtained from *meso*-3,4-bis(4-fluorophenyl)-1,6-bis(2-hydroxy-3-fluorophenyl)-2,5-diazahexa-1,5-diene (**7**) (0.19 mmol, 93 mg) and potassium tetrachloroplatinate (0.19 mmol, 79 mg). Yield: 79 mg (0.11 mmol, 61%) of a yellow powder. ^{1}H NMR (DMSO-d_6): $\delta = 5.62$ (s, 2H, C*H*); 6.51–6.64 (m, 2H, Ar*H*-5); 7.06–7.19 (t, $^3J = 8.70$ Hz, 4H, Ar′*H*-3, Ar′*H*-5); 7.19–7.39 (m, 6H, Ar*H*-6, Ar′*H*-2, Ar′*H*-6); 7.38–7.52 (m, 2H, Ar*H*-3); 8.35 (s, 2H, NC*H*). HRMS (+)-ESI *m*/*z* [M + Na]$^+$ calcd for $C_{28}H_{18}F_4N_2NaO_2Pt^+$: 708.0850; found: 708.0852.

*5.2.2.8. [meso-3,4-Bis(4-fluorophenyl)-1,6-bis(2-hydroxy-4-fluorophenyl)-2,5-diazahexa-1,5-diene]platinum(II) [**8-Pt**].* **8-Pt** was obtained from *meso*-3,4-bis(4-fluorophenyl)-1,6-bis(2-hydroxy-4-

fluorophenyl)-2,5-diazahexa-1,5-diene (**8**) (0.19 mmol, 94 mg) and potassium tetrachloroplatinate (0.19 mmol, 79 mg). Yield: 79 mg (0.11 mmol, 61%) of a yellow powder. ^{1}H NMR (DMSO-d_6): $\delta = 5.55$ (s, 2H, C*H*); 6.46–6.54 (m, 2H, Ar*H*-5); 6.73–6.80 (dd, $^3J = 12.06$ Hz, $^4J = 2.27$ Hz, 2H, Ar*H*-3); 7.06–7.15 (t, $^3J = 8.81$ Hz, 4H, Ar′*H*-3, Ar′*H*-5); 7.18–7.28 (m, 4H, Ar′*H*-2, Ar′*H*-6); 7.50–7.58 (m, 2H, Ar*H*-6); 8.26 (s, 2H, NC*H*). HRMS (+)-ESI *m/z* [M + Na]$^+$ calcd for $C_{28}H_{18}F_4N_2NaO_2Pt^+$: 708.0850; found: 708.0866.

*5.2.2.9. [meso-3,4-Bis(4-fluorophenyl)-1,6-bis(2-hydroxy-5-fluorophenyl)-2,5-diazahexa-1,5-diene]platinum(II) [**9-Pt**].* **9-Pt** was obtained from *meso*-3,4-bis(4-fluorophenyl)-1,6-bis(2-hydroxy-5-fluorophenyl)-2,5-diazahexa-1,5-diene (**9**) (0.16 mmol, 77 mg) and potassium tetrachloroplatinate (0.16 mmol, 65 mg). Yield: 93 mg (0.13 mmol, 82%) of a dark yellow powder. ^{1}H NMR (DMSO-d_6): $\delta = 5.56$ (s, 2H, C*H*); 6.94–7.03 (dd, $^3J = 9.27$ Hz, $^4J = 4.81$ Hz, 2H, Ar*H*-3); 7.07–7.16 (t, $^3J = 8.82$ Hz, 4H, Ar′*H*-3, Ar′*H*-5); 7.18–7.25 (m, 4H, Ar′*H*-2, Ar′*H*-6); 7.30–7.46 (m, 4H, Ar*H*-4, Ar*H*-6); 8.29 (s, 2H, NC*H*). HRMS (+)-ESI *m/z* [M + Na]$^+$ calcd for $C_{28}H_{18}F_4N_2NaO_2Pt^+$: 708.0850; found: 708.0853.

*5.2.2.10. [meso-3,4-Bis(4-fluorophenyl)-1,6-bis(2-hydroxy-6-fluorophenyl)-2,5-diazahexa-1,5-diene]platinum(II) [**10-Pt**].* **10-Pt** was obtained from *meso*-3,4-bis(4-fluorophenyl)-1,6-bis(2-hydroxy-6-fluorophenyl)-2,5-diazahexa-1,5-diene (**10**) (0.13 mmol, 64 mg) and potassium tetrachloroplatinate (0.13 mmol, 53 mg). Yield: 48 mg (0.07 mmol, 54%) of a yellow powder. ^{1}H NMR (DMSO-d_6): $\delta = 5.67$ (s, 2H, C*H*); 6.37–6.48 (dd, $^3J = 10.90$ Hz, $^4J = 8.05$ Hz, 2H, Ar*H*-5); 6.81–6.90 (d, $^3J = 8.79$ Hz, 2H, Ar*H*-3); 7.08–7.20 (t, $^3J = 8.73$ Hz, 4H, Ar′*H*-3, Ar′*H*-5); 7.20–7.31 (m, 4H, Ar′*H*-2, Ar′*H*-6); 7.39–7.50 (m, 2H, Ar*H*-4); 8.46 (s, 2H, NC*H*). HRMS (+)-ESI *m/z* [M + Na]$^+$ calcd for $C_{28}H_{18}F_4N_2NaO_2Pt^+$: 708.0850; found: 708.0853.

5.3. X-ray Crystallography

The intensities for the X-ray determinations were collected on an STOE IPDS 2T instrument with Mo Kα radiation ($\lambda = 0.71073$ Å) at 200 K. Standard procedures were applied for data reduction and absorption correction. Structure solution and refinement were performed with SHELXS97 and SHELXL97 [27]. Hydrogen atom positions were calculated for idealized positions and treated with the "riding model" option of SHELXL. More details on data collections and structure calculations are contained in Table 1. Selected bond lengths and angles are summarized in Table 3.

Table 3
Selected bond lengths (Å) and angles (°) in **9-Pt**.

Pt(1)–N(1)	1.922(7)	Pt(1)–N(2)	1.932(7)
Pt(1)–O(1)	1.959(6)	Pt(1)–O(2)	2.022(6)
N(1)–C(8)	1.28(1)	N(1)–C(9)	1.511(9)
N(2)–C(14)	1.50(1)	N(2)–C(15)	1.28(1)
O(1)–C(1)	1.32(1)	O(2)–C(21)	1.317(9)
N(1)–Pt(1)–N(2)	85.4(3)	N(1)–Pt(1)–O(1)	94.9(3)
N(1)–Pt(1)–O(2)	178.8(3)	N(2)–Pt(1)–O(1)	179.1(3)
N(2)–Pt(1)–O(2)	93.9(3)	O(1)–Pt(1)–O(2)	85.0(3)

5.4. Cytotoxicity

The human MCF-7 and MDA-MB 231 breast cancer as well as HT-29 colon cancer cell lines were obtained from the American Type Culture Collection. The cells were maintained as a monolayer culture in L-glutamine containing Dulbecco's modified Eagle's medium (DMEM) with 4.5 g/L glucose (PAA Laboratories, Austria), supplemented with 5% foetal bovine serum (FBS; Biochrom, Germany) in a humidified atmosphere (5% CO_2) at 37 °C. The experiments were performed according to established procedures with some modifications [26,28,29]. In 96 well plates, 100 μL of a cell suspension in culture medium at 7500 cells/mL (MCF-7 and MDA-MB 231) or 3000 cells/mL (HT-29) were plated into each well and were incubated for three days under cell culture conditions. After the addition of various concentrations of the test compounds, cells were incubated for up to appropriate incubation time. Then the medium was removed, the cells were fixed with glutardialdehyde solution 1% and stored under phosphate buffered saline (PBS) at 4 °C. Cell biomass was determined by a crystal violet staining, followed by extracting of the bound dye with ethanol and a photometric measurement at 590 nm. Mean values were calculated and the effects of the compounds were expressed as % Treated/Control$_{corr}$ values according to the following equation:

$$T/C_{corr}[\%] = \frac{T - C_0}{C - C_0} \times 100$$

(C_0 control cells at the time of compound addition; C control cells at the time of test end; T probes/samples at the time of test end). The IC_{50} value was determined as the concentration causing 50% inhibition of cell proliferation and calculated as mean of at least two independent experiments (OriginPro 8).

Acknowledgement

This work was supported by the Deutsche Forschungsgemeinschaft (DFG) within FOR 630 "Biological function of organometallic compounds".

Appendix. Supplementary data

Supplementary data associated with this article can be found, in the online version, at doi:10.1016/j.ejmech.2012.03.053.

References

[1] B. Rosenberg, L. Van Camp, T. Krigas, Inhibition of cell division in *Escherichia coli* by electrolysis products from a platinum electrode, Nature 205 (1965) 698–699.
[2] N.J. Wheate, S. Walker, G.E. Craig, R. Oun, The status of platinum anticancer drugs in the clinic and in clinical trials, Dalton Trans. 39 (2010) 8113–8127.
[3] L. Kelland, The resurgence of platinum-based cancer chemotherapy, Nat. Rev. Cancer 7 (2007) 573–584.
[4] Z.H. Siddik, Cisplatin: mode of cytotoxic action and molecular basis of resistance, Oncogene 22 (2003) 7265–7279.
[5] L.P. Martin, T.C. Hamilton, R.J. Schilder, Platinum resistance: the role of DNA repair pathways, Clin. Cancer Res. 14 (2008) 1291–1295.
[6] R. Gust, W. Beck, G. Jaouen, H. Schönenberger, Optimization of cisplatin for the treatment of hormone dependent tumoral diseases. Part 1: use of steroidal ligands, Coord. Chem. Rev. 253 (2009) 2742–2759.
[7] R. Gust, W. Beck, G. Jaouen, H. Schönenberger, Optimization of cisplatin for the treatment of hormone-dependent tumoral diseases. Part 2: use of non-steroidal ligands, Coord. Chem. Rev. 253 (2009) 2760–2779.
[8] C. Cassino, E. Gabano, M. Ravera, G. Cravotto, G. Palmisano, A. Vessières, G. Jaouen, S. Mundwiler, R. Alberto, D. Osella, Platinum(II) and technetium(I) complexes anchored to ethynylestradiol: a way to drug targeting and delivery, Inorg. Chim. Acta 357 (2004) 2157–2166.
[9] S. Chaney, The chemistry and biology of platinum complexes with the 1,2-diaminocyclohexane carrier ligand (review), Int. J. Oncol. 6 (1995) 1291–1305.
[10] A. Ray, S. Banerjee, G.M. Rosair, V. Gramlich, S. Mitra, Variation in coordinative property of two different N_2O_2 donor Schiff base ligands with nickel(II) and cobalt(III) ions: characterisation and single crystal structure elucidation, Struct. Chem. 19 (2008) 459–465.
[11] A. Hille, R. Gust, Relationship between anticancer activity and stereochemistry of saldach ligands and their iron(III) complexes, Arch. Pharm. 342 (2009) 625–631.
[12] A. Hille, I. Ott, A. Kitanovic, I. Kitanovic, H. Alborzinia, E. Lederer, S. Wölfl, N. Metzler-Nolte, S. Schäfer, W. Sheldrick, C. Bischof, U. Schatzschneider,

R. Gust, [*N*,*N*′-Bis(salicylidene)-1,2-phenylenediamine]metal complexes with cell death promoting properties, J. Biol. Inorg. Chem. 14 (2009) 711–725.
[13] A. Hille, R. Gust, Influence of methoxy groups on antiproliferative effects of [Fe^{III}(salophene-OMe)Cl] complexes, Eur. J. Med. Chem. 45 (2010) 5486–5492.
[14] R. Gust, I. Ott, D. Posselt, K. Sommer, Development of cobalt(3,4-diarylsalen) complexes as tumor therapeutics, J. Med. Chem. 47 (2004) 5837–5846.
[15] R. Gust, H. Schönenberger, Third generation antitumor platinum(II) complexes of the [1-(fluoro/difluorophenyl)-2-phenylethylenediamine]platinum(II) type, Arch. Pharm. 328 (1995) 595–603.
[16] F. Vögtle, E. Goldschmitt, Die Diaza-Cope-Umlagerung, Chem. Ber. 109 (1976) 1–40.
[17] F. Vögtle, E. Goldschmitt, [3,3]-Sigmatropic reactions in the *N*,*N*′-dimethyleneethylenediamine system, Angew. Chem., Int. Ed. Engl. 12 (1973) 767–768.
[18] F. Vögtle, E. Goldschmitt, Dynamic stereochemistry of the degenerate diaza-Cope rearrangement, Angew. Chem., Int. Ed. Engl. 13 (1974) 480–482.
[19] M. Jennerwein, R. Gust, R. Müller, H. Schönenberger, J. Engel, M.R. Berger, D. Schmähl, S. Seeber, R. Osieka, G. Atassi, D. Maréchal-De Bock, Tumor inhibiting properties of stereoisomeric [1,2-bis(3-hydroxyphenyl)ethylenediamine]dichloroplatinum(II)-complexes. Part I: synthesis, Arch. Pharm. 322 (1989) 25–29.
[20] W.L. Tong, L.M. Lai, M.C. Chan, Platinum(II) Schiff base as versatile phosphorescent core component in conjugated oligo(phenylene-ethynylene)s, Dalton Trans. (2008) 1412–1414.
[21] J. Chin, F. Mancin, N. Thavarajah, D. Lee, A. Lough, D.S. Chung, Controlling diaza-Cope rearrangement reactions with resonance-assisted hydrogen bonds, J. Am. Chem. Soc. 125 (2003) 15276–15277.
[22] H. Kim, Y. Nguyen, C.P. Yen, L. Chagal, A.J. Lough, B.M. Kim, J. Chin, Stereospecific synthesis of C2 symmetric diamines from the mother diamine by resonance-assisted hydrogen-bond directed diaza-Cope rearrangement, J. Am. Chem. Soc. 130 (2008) 12184–12191.
[23] C.-M. Che, C.-C. Kwok, S.-W. Lai, A.F. Rausch, W.J. Finkenzeller, N. Zhu, Y. Hartmut, Photophysical properties and OLED applications of phosphorescent platinum(II) Schiff base complexes, Chem. Eur. J. 16 (2010) 233–247.
[24] W. Sawodny, U. Thewalt, E. Potthoff, R. Ohl, [*N*,*N*′-Bis(salicylidene)ethylenediaminato-*N*,*N*′,*O*,*O*′]platinum(II), Acta Crystallogr. C55 (1999) 2060–2061.
[25] C.-M. Che, S.-C. Chan, H.-F. Xiang, C.M. Chan, Y. Liu, Y. Wang, Tetradentate Schiff base platinum(II) complexes as a new class of phosphorescent materials for high-efficiency and white-light electroluminescent devices, Chem. Commun. (2004) 1484–1485.
[26] G. Bernhardt, H. Reile, H. Birnböck, T. Spruss, H. Schönenberger, Standardized kinetic microassay to quantify differential chemosensitivity on the basis of proliferative activity, J. Cancer Res. Clin. Oncol. 118 (1992) 35–43.
[27] G.M. Sheldrick, SHELXS-97 and SHELXL-97, Programs for the Solution and Refinement of Crystal Structures, University of Goettingen, Goettingen, Germany, 1997.
[28] H. Reile, H. Birnböck, G. Bernhardt, T. Spruss, H. Schönenberger, Computerized determination of growth kinetic curves and doubling times from cells in microculture, Anal. Biochem. 187 (1990) 262–267.
[29] W. Liu, J. Zhou, K. Bensdorf, H. Zhang, H. Liu, Y. Wang, H. Qian, Y. Zhang, A. Wellner, G. Rubner, W. Huang, C. Guo, R. Gust, Investigations on cytotoxicity and anti-inflammatory potency of licofelone derivatives, Eur. J. Med. Chem. 46 (2011) 907–913.